Table II. Effects of Reconstitution Medium on β-GA Aggregation Above T_g for 0.33 Trehalose Formulation

Additives in Reconstitution Medium	Peak Height for Monomeric β-GA (Relative to Solution Prior to Freeze Drying)			
	After Freeze Drying		After 9 h-storage at 90°C	
None	0.99	(0.01)	0.74	(0.03)
Dextran Sulfate	1.00	(0.00)	0.74	(0.01)
2-hydroxylpropyl-β-cyclodextrin	0.98	(0.00)	0.73	(0.01)
Poly-L-lysine	0.98	(0.01)	0.74	(0.01)
Pluronic	1.00	(0.01)	0.76	(0.02)

0.5% additives
Values in brackets represent standard deviation (n=3)

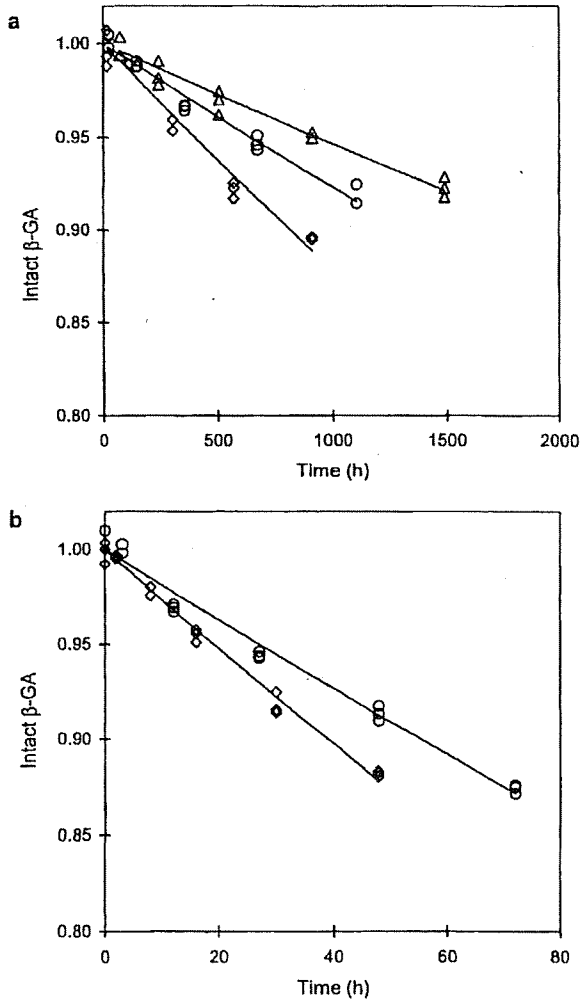

Fig. 2. Time courses of aggregation of β-GA lyophilized with sucrose (△), trehalose (○) or stachyose (◇). (a) aggregation at 50°C and excipient fraction of 0.33. (b) aggregation at 80°C and excipient fraction of 0.5.

Excipient-Fraction Dependence of β-GA Aggregation Rate

Figure 4 shows the dependence of t_{90} on the weight fraction of excipient at temperatures below T_g (50°C) and above T_g (80°C). As the weight fraction of excipient increased, t_{90} increased for all formulations. The values of t_{90} for the sucrose formulation in the amorphous state could not be determined at fractions above 0.5 at 50°C or above 0.33 at 80°C, because crystallization occurred during storage (crystallization was confirmed by the lack of crystallization peak in DSC thermograms). The t_{90} observed for β-GA aggregation showed a log-linear dependence on the excipient fraction, as reported for other proteins (11,12).

Figure 5 shows the water content and T_g determined for the lyophilized β-GA formulations with various weight fractions of trehalose, sucrose or stachyose. It has often been reported that lyophilized proteins without excipients do not show a distinct change in heat capacity in DSC thermograms. The T_g of lyophilized β-GA alone could not be determined in the dry state, but it could be estimated at 12% RH from small changes in heat capacity (Fig. 6). The T_g value determined at 12% RH depended on the excipient fraction (Fig. 5); T_g decreased with increasing excipient fraction from 0 to 0.3. Only a single T_g was observed in the range of excipient fractions from 0 to 0.3 for all formulations, suggesting that these formulations are a single glassy phase on levels detectable by DSC.

As shown in Figs. 4 and 5, the rank order of t_{90} at a certain excipient fraction was sucrose > trehalose > stachyose, whereas that of T_g of β-GA formulations was sucrose < trehalose < stachyose. The value of t_{90} increased significantly with increasing excipient fraction, even at small excipient fractions, in which T_g decreased significantly with increasing excipient fraction. These findings indicate that β-GA aggregation rate is not primarily related to ($T-T_g$).

Figure 7 shows the amount of monomeric β-GA remaining after freeze drying with sucrose, trehalose or stachyose. Significant changes were observed at an excipient fraction of 0.09 for all formulations. The stachyose formulation exhibited the largest degree of β-GA aggregation during freeze drying. This finding suggests that freeze-drying processes cause changes in protein conformation at differing degrees between excipients, which in turn leads to the differences in β-GA aggregation rate observed between excipients. FT-IR is known to be useful for detecting changes in protein conformation produced during the freeze-drying process (17). Figure 8 compares the second derivative FT-IR

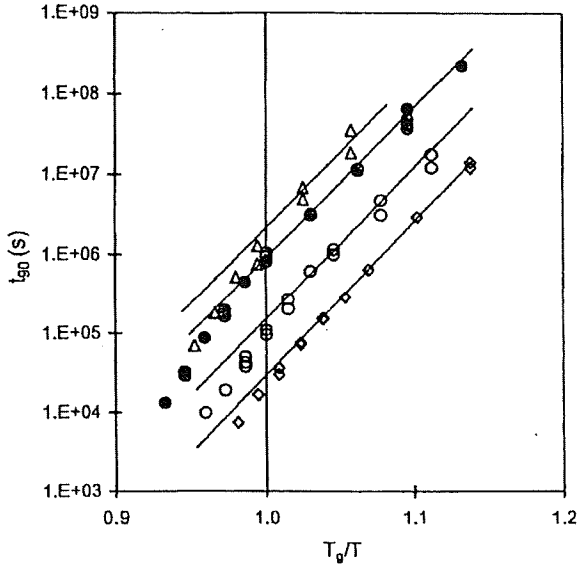

Fig. 3. T/T_g-dependence of t_{90} for aggregation of β-GA lyophilized with sucrose (△), trehalose (○●) or stachyose (◇). The weight fraction of excipient : 0.33 (△○◇) and 0.5 (●).

spectra between the sucrose, trehalose and stachyose formulations. Significant differences in spectra were not observed between the excipients, and the differences in β-GA aggregation rate observed between the excipients could not be attributed to differences in protein secondary structure. It is known that changes in the tertiary structure of protein molecules created during freeze-drying processes can lead to

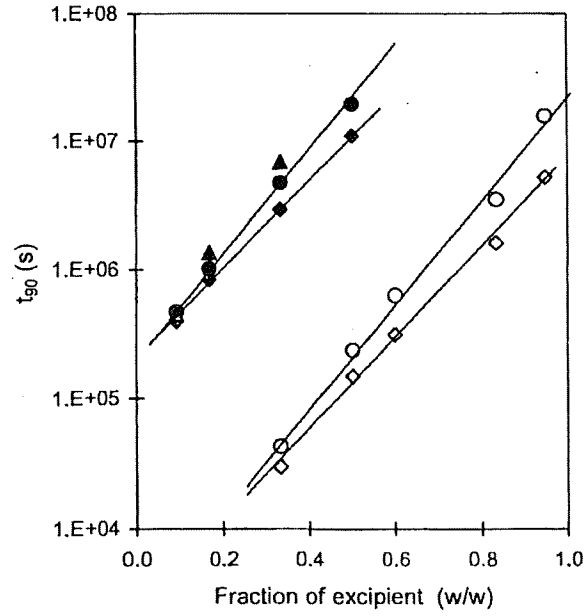

Fig. 4. Dependence of t_{90} on the weight fraction of excipient. The value of t_{90} was determined at 80°C and 12%RH for trehalose (○) and stachyose (◇), and at 50°C and 12%RH for trehalose (●), sucrose (▲) and stachyose (◆).

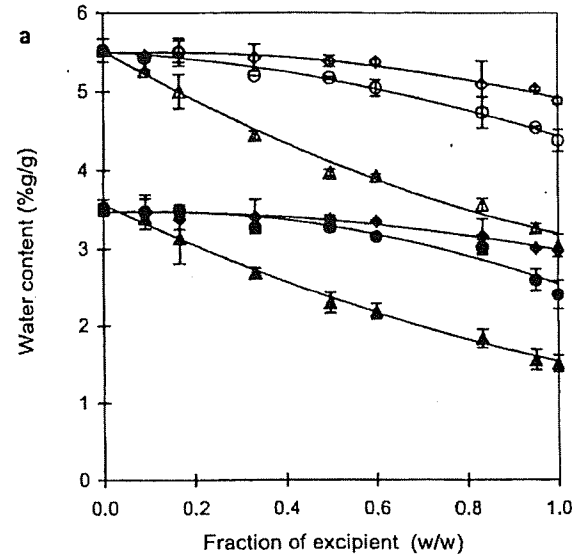

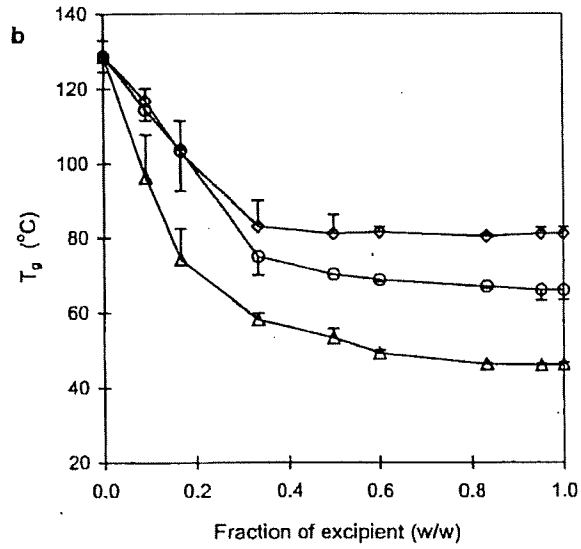

Fig. 5. Water content (a) and T_g (b) of lyophilized β-GA formulations containing trehalose (○●), sucrose (△▲), or stachyose (◇◆) as a function of the weight fraction of excipient. (a) *closed symbols*: 10%RH; *open symbols*: 20%RH. 25°C. (b) 12%RH. sd (n=3).

protein aggregation during storage. A possibility that a tertiary structural change is responsible for the differences in β-GA aggregation rate observed between the excipients cannot be excluded.

Significance of Local Mobility, as Determined by $T_{1\rho}$ of β-GA Carbonyl Carbon, and Structural Relaxation in Protein Aggregation

It is generally considered that the rate of protein aggregation, an intermolecular reaction, is mainly determined by structural relaxation that allows for large-scale

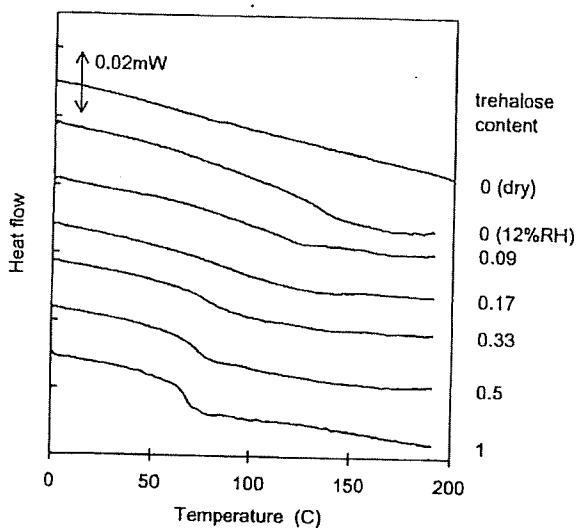

Fig. 6. DSC thermogram for β-GA lyophilized with various weight fractions of trehalose.

diffusion of reactants. From the finding that the t_{90} versus T_g/T plots for the lyophilized β-GA formulations exhibited a change in slope around T_g, β-GA aggregation rate appeared to correlate with structural relaxation. Although β-GA aggregation rate was not related to $(T-T_g)$, this may be explained by assuming that the fragility and fictive temperature of the formulation vary with the excipient. Because the structural relaxation times of the β-GA formulations were not determined in this study, correlations between β-GA aggregation rate and structural relaxation could not be elucidated.

Meanwhile, the local mobility of β-GA was determined by $T_{1\rho}$ of β-GA carbonyl carbon. Figure 9 shows the time course of rotating-frame spin-lattice relaxation at 25°C and 12% RH for the carbonyl carbon of β-GA lyophilized with sucrose, trehalose or stachyose at an excipient fraction of 0.5.

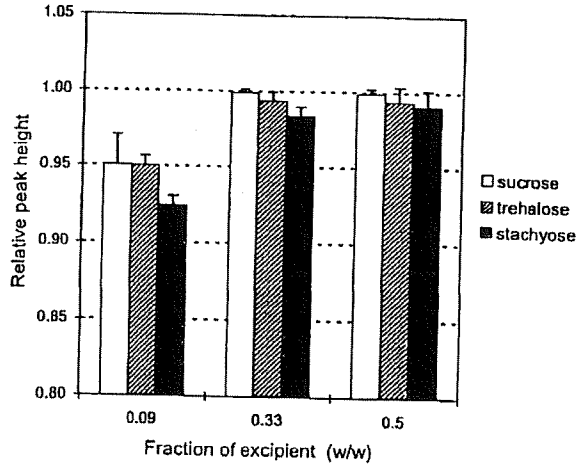

Fig. 7. Ratio of monomeric β-GA remaining after freeze drying with sucrose, trehalose or stachyose. *Bars* represent standard deviation (n=3).

Spin-lattice relaxation was significantly retarded by the addition of excipient. Sucrose resulted in the largest degree of retardation, and there were no significant differences in the degree of retardation between the trehalose and stachyose formulations. The time course of spin-lattice relaxation was describable with a bi-exponential equation including two different $T_{1\rho}$ values. The longer $T_{1\rho}$ value was estimated by curve fitting using a shorter $T_{1\rho}$ of 9 ms and a proportion of 13% for carbonyl carbons with the shorter $T_{1\rho}$. Figure 10 shows the estimates for the longer $T_{1\rho}$ of the dominating proportion, plotted as a function of the excipient fraction. The $T_{1\rho}$ for the sucrose formulation increased significantly with excipient fraction. For the stachyose formulation, in contrast, increases in $T_{1\rho}$ were not significant at an excipient fraction of 0.09, and $T_{1\rho}$ was less than in the sucrose formulation at higher excipient fractions. $T_{1\rho}$ for the trehalose formulation exhibited intermediate behavior when compared to the sucrose and stachyose formulations. The rank order of the ability of excipients to decrease the local

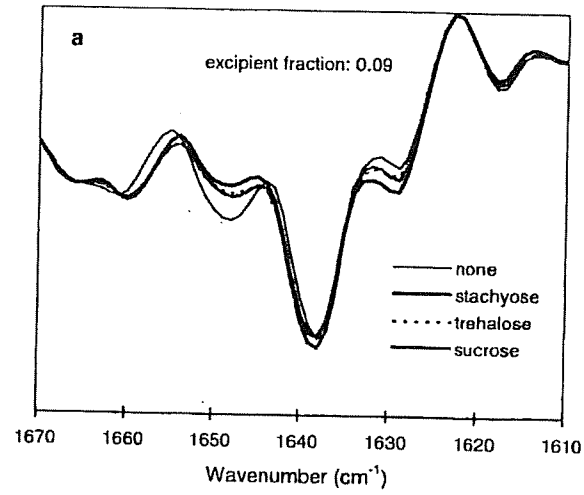

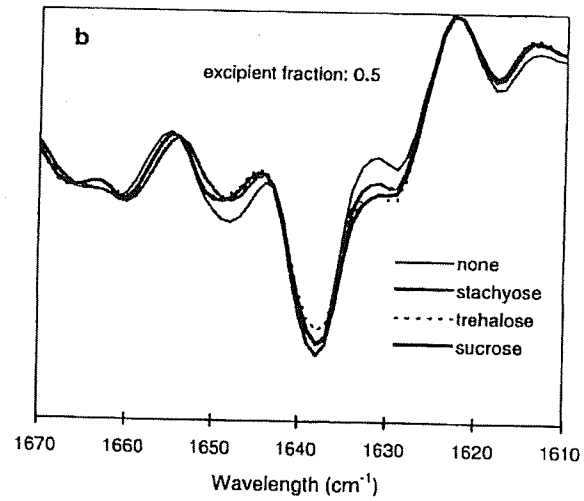

Fig. 8. Second derivative FT-IR spectra for β-GA lyophilized with sucrose, trehalose or stachyose of 0.09 (a) and 0.5 fractions (b).

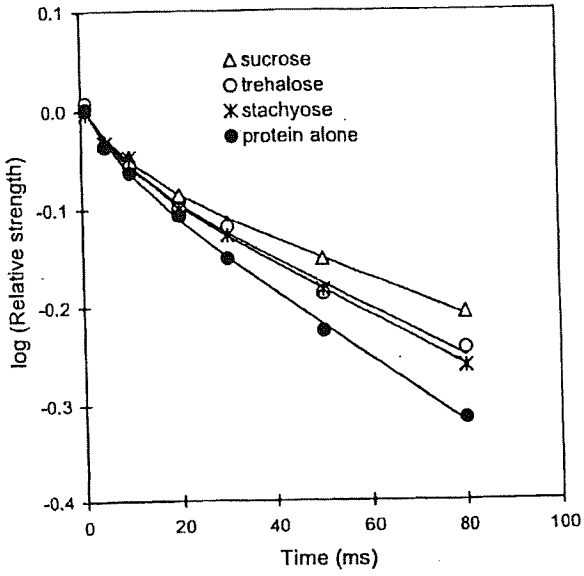

Fig. 9. Time course of spin-lattice relaxation at 25°C and 12%RH for carbonyl carbon of β-GA lyophilized with sucrose, trehalose or stachyose. The weight fraction of excipient : 0.5.

mobility of β-GA appeared to be the same as the rank order of their ability to decrease aggregation rate. This finding suggests that local mobility is a primary factor that affects the stability of lyophilized β-GA formulations; sucrose more potently inhibits local mobility of β-GA, and thus more strongly inhibits β-GA aggregation.

Local mobility is generally considered to follow Arrhenius kinetics. If local mobility is mainly responsible for β-GA aggregation, the temperature dependence of t_{90} should not show a change in slope around T_g. The non-Arrhenius temperature dependence observed for the t_{90} of β-GA aggregation, which is considered to be governed by local mobility, may be explained by assuming that local mobility of protein is coupled with structural relaxation. For bovine serum γ-globulin, the local mobility of protein, as measured by the laboratory-frame spin-lattice relaxation time (T_1) of protein carbonyl carbon, exhibited Arrhenius temperature dependence when lyophilized without excipient (18). When lyophilized with dextran, in contrast, the local mobility of protein exhibited a change in the slope of temperature dependence around the T_{mc} (T_g determined by NMR relaxation measurement), as did local mobility of dextran, as measured by T_1 of dextran methine carbon. These findings suggested that the local mobility of protein was coupled with the structural relaxation of lyophilized solids. The same may be said for the local mobility of protein and structural relaxation of β-GA lyophilized with sucrose, trahalose or stachyose. The local mobility of β-GA may exhibit Arrhenius temperature dependence in the absence of excipient. Upon the addition of excipient, local mobility may become to be coupled with structural relaxation, and the temperature dependence of protein local mobility may become to deviate from Arrhenius behavior.

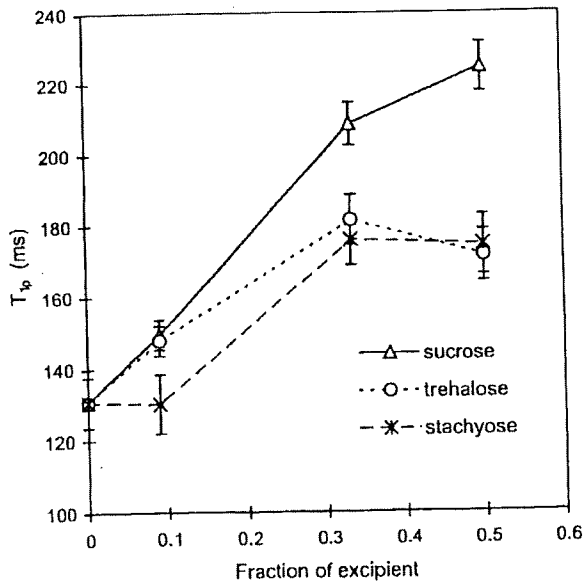

Fig. 10. Effect of weight fraction of excipient on $T_{1\rho}$ of carbonyl carbon at 25°C and 12%RH for β-GA lyophilized with sucrose, trehalose or stachyose

The great increase in t_{90} with increasing excipient fraction observed for β-GA aggregation rate, as indicated by log-linear dependence on the excipient fraction, may be attributed mainly to the effect of excipient inhibiting protein local mobility in addition to the effect of excipient diluting protein molecules.

CONCLUSION

The aggregation rate of β-GA lyophilized with sucrose, trehalose or stachyose unexpectedly correlated with the local mobility of β-GA rather than with ($T-T_g$). An increase in the weight fraction of excipient appeared to increase the effects of excipient decreasing local mobility, resulting in increases in the stability of β-GA. Sucrose exhibited the most intense stabilizing effect due to the most intense ability to inhibit local protein mobility during storage.

REFERENCES

1. M. J. Pikal. Chemistry in solid amorphous matrices: implication for biostabilization. In H. Levine (ed.), *Amorphous Food and Pharmaceutical Systems*, The Royal Society of Chemistry, Cambridge, UK, 2002, pp. 257–272.
2. S. Yoshioka, and Y. Aso. Correlations between molecular mobility and chemical stability during storage of amorphous pharmaceuticals. *J. Pharm. Sci.* in press (2006).
3. M. J. Pikal, K. M. Dellerman, M. L. Roy, and R. M. Riggin. The effects of formulation variables on the stability of freeze-dried human growth hormone. *Pharm. Res.* 8:427–436 (1991).
4. C. Schebor, M. P. Buera, and J. Chirife. Glassy state in relation to thermal inactivation of the enzyme invertase in amorphous dried matrices of trehalose, maltodextrin and PVP. *J. Food Eng.* 30:269–282 (1996).
5. S. J. Prestrelski, K. A. Pikal, and T. Arakawa. Optimization of lyophilization conditions for recombinant human interleukin-2

by dried-state conformational analysis using fourier-transform infrared spectroscopy. *Pharm. Res.* **12**:1250–1259 (1995).
6. S. Yoshioka, Y. Aso, and S. Kojima. Dependence of molecular mobility and protein stability of freeze-dried γ-globulin formulations on the molecular weight of dextran. *Pharm. Res.* **14**:736–741 (1997).
7. S. P. Duddu, and P. R. Dal Monte. Effect of glass transition temperature on the stability of lyophilized formulations containing a chimeric therapeutic monoclonal antibody. *Pharm. Res.* **14**:591–595 (1997).
8. S. Yoshioka, Y. Aso, and S. Kojima. Determination of molecular mobility of lyophilized bovine serum albumin and γ-globulin by solid state ^{1}H-NMR and relation to aggregation-susceptibility. *Pharm. Res.* **13**:926–930 (1996).
9. S. Yoshioka, Y. Aso, and S. Kojima. Softening temperature of lyophilized bovine serum albumin and γ-globulin as measured by spin-spin relaxation time of protein protons. *J. Pharm. Sci.* **86**:470–474 (1997).
10. S. Yoshioka, S. Tajima, Y. Aso, and S. Kojima. Inactivation and aggregation of β-galactosidase in lyophilized formulation described by Kohlrausch-Williams-Watts stretched exponential function. *Pharm. Res.* **20**:1655–1660 (2003).
11. L. Chang, D. Shepherd, J. Sun, D. Ouellette, K. L. Grant, X. Tang, and M. J. Pikal. Mechanism of protein stabilization by sugars during freeze-drying and storage: native structure preservation, specific interaction, and/or immobilization in a glassy matrix? *J. Pharm. Sci.* **94**:1427–1444 (2005).
12. L. Chang, D. Shepherd, J. Sun, X. Tang, and M. J. Pikal. Effect of sorbitol and residual moisture on the stability of lyophilized antibodies: implications for the mechanism of protein stabilization in the solid state. *J. Pharm. Sci.* **94**:1445–1455 (2005).
13. S. Yoshioka, Y. Aso, S. Kojima, and T. Tanimoto. Effect of polymer excipients on the enzyme activity of lyophilized bilirubin oxidase and β-galactosidase formulations. *Chem. Pharm. Bull.* **48**:283–285 (2000).
14. S. Yoshioka, Y. Aso, and S. Kojima. Usefulness of Kohlrausch-Williams-Watts stretched exponential function to describe protein aggregation in lyophilized formulations and temperature dependence of near the glass transition temperature. *Pharm. Res.* **18**:256–260 (2001).
15. S. Yoshioka, Y. Aso, and S. Kojima. The effect of excipients on the molecular mobility of lyophilized formulations, as measured by glass transition temperature and NMR relaxation-based critical mobility temperature. *Pharm. Res.* **16**:135–140 (1999).
16. M. Z. Zhang, K. Pikal, T. Nguyen, T. Arakawa, and S. J. Prestrelski. The effect of the reconstitution medium on aggregation of lyophilized recombinant interleukin-2 and ribonuclease A. *Pharm .Res.* **13**:643–646 (1996).
17. S. J. Prestrelski, T. Arakawa, and J. Carpenter. Separation of freezing- and drying-induced denaturation of lyophilized proteins using stress-specific stabilization. *Arch. Biochem. Biophys.* **303**:465–473 (1993).
18. S. Yoshioka, Y. Aso, S. Kojima, S. Sakurai, T. Fujiwara, and H. Akutsu. Molecular mobility of protein in lyophilized formulations linked to the molecular mobility of polymer excipients, as determined by high resolution ^{13}C solid-state NMR. *Pharm. Res.* **16**:1621–1625 (1999).

Available online at www.sciencedirect.com
ScienceDirect
ELSEVIER
International Journal of Pharmaceutics 336 (2007) 191–195
INTERNATIONAL JOURNAL OF PHARMACEUTICS
www.elsevier.com/locate/ijpharm

Note

Crystallization rate of amorphous nifedipine analogues unrelated to the glass transition temperature

Tamaki Miyazaki*, Sumie Yoshioka, Yukio Aso, Toru Kawanishi

National Institute of Health Sciences, 1-18-1 Kamiyoga, Setagaya-ku, Tokyo 158-0851, Japan

Received 14 August 2006; received in revised form 12 October 2006; accepted 18 November 2006
Available online 28 November 2006

Abstract

To examine the relative contributions of molecular mobility and thermodynamic factor, the relationship between glass transition temperature (T_g) and the crystallization rate was examined using amorphous dihydropyridines (nifedipine (NFD), *m*-nifedipine (*m*-NFD), nitrendipine (NTR) and nilvadipine (NLV)) with differing T_g values. The time required for 10% crystallization, t_{90}, was calculated from the time course of decreases in the heat capacity change at T_g. The t_{90} of NLV and NTR decreased with decreases in T_g associated with water sorption. The t_{90} versus T_g/T plots almost overlapped for samples of differing water contents, indicating that the crystallization rate is determined by molecular mobility as indicated by T_g. In contrast, differences in the crystallization rate between these four drugs cannot be explained only by molecular mobility, since the t_{90} values at a given T_g/T were in the order: NLV > NTR > NFD ≈ *m*-NFD. A lower rate was obtained for amorphous drugs with lower structural symmetry and more bulky functional groups, suggesting that these factors are also important. Furthermore, the crystallization rate of NTR in solid dispersions with poly(vinylpyrrolidone) (PVP) and hydroxypropyl methylcellulose (HPMC) decreased to a greater extent than expected from the increased T_g. This also suggests that factors other than molecular mobility affect the crystallization rate.

Keywords: Crystallization; Amorphous state; Nifedipine; Glass transition; Molecular mobility; Excipients

Preparation of poorly water-soluble pharmaceuticals into amorphous forms improves their solubility. However, amorphous solids are physically unstable because of their high energy state, and crystallization during storage presents a problem. The process of crystallization is known to comprise two major steps: nucleation and crystal growth, and the rates are generally governed by molecular mobility affecting the diffusion rate of molecules and thermodynamic factors such as the Gibbs free energy and nucleus/amorphous interfacial energy (Salcki-Gerhardt and Zografi, 1994; Hancock and Zografi, 1997; Rodríguez-Hornedo and Murphy, 1999; Andronis and Zografi, 2000; Ngai et al., 2000). Our previous studies demonstrated that the overall crystallization rate of nifedipine (NFD) for both the amorphous pure drug and solid dispersions with poly(vinylpyrrolidone) (PVP) had similar temperature dependence as the mean relaxation time calculated using the Adam-Gibbs-Vogel equation, suggesting that the molecular mobility of amorphous pharmaceuticals was one of the important factors affecting the crystallization rate (Aso et al., 2001, 2004). However, the crystallization rate of amorphous pharmaceuticals cannot be determined only by molecular mobility, as it has been reported that the susceptibility to crystallization of pharmaceuticals possessing quite different thermodynamic properties does not follow the order of the decrease in the glass transition temperature (T_g) (Zhou et al., 2002).

The purpose of the present study is to discuss the relative contributions of the molecular mobility and thermodynamic factors to the crystallization rates of dihydropyridines with different substituents, including NFD, *m*-nifedipine (*m*-NFD), nitrendipine (NTR) and nilvadipine (NLV) (Fig. 1). The overall crystallization rates of these drugs in the pure amorphous solids were measured under various relative humidity (RH) conditions to elucidate the effects of the substituents and water content on the crystallization rate. The crystallization rate of NTR was also determined in solid dispersions containing polymers (PVP and hydroxypropyl methylcellulose (HPMC)). Although some

* Corresponding author. Tel.: +81 3 3700 1141; fax: +81 3 3707 6950.
E-mail addresses: miyazaki@nihs.go.jp (T. Miyazaki), yoshioka@nihs.go.jp (S. Yoshioka), aso@nihs.go.jp (Y. Aso), kawanish@nihs.go.jp (T. Kawanishi).

0378-5173/$ – see front matter © 2006 Elsevier B.V. All rights reserved.
doi:10.1016/j.ijpharm.2006.11.052

	abbreviation	R_1	R_2	R_3	R_4
nifedipine	[NFD]	CH_3	CH_3	NO_2	H
m-nifedipine	[m-NFD]	CH_3	CH_3	H	NO_2
nitrendipine	[NTR]	CH_3	C_2H_5	H	NO_2
nilvadipine	[NLV]	CN	$(CH_3)_2CH$	H	NO_2

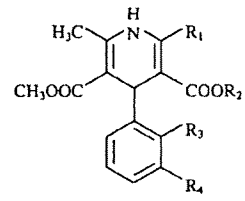

Fig. 1. Chemical structures of dihydropyridines.

papers have dealt with the crystallization of NTR and NLV in solid dispersions (Hirasawa et al., 2003a,b, 2004; Wang et al., 2005, 2006), few data are available that allow quantitative discussion about the relationship between molecular mobility and crystallization rates.

NFD and HPMC (USP grade) were purchased from Sigma Chemical Co. NTR, *m*-NFD and PVP (weight average molecular weight of 40000) were obtained from Wako Pure Chemical Industries Ltd. NLV was kindly supplied by Astellas Pharma Inc. The amorphous NFD, *m*-NFD, NTR, NLV and NTR solid dispersions with PVP and HPMC were prepared by melt quenching in the cell of a differential scanning calorimeter (DSC2920, TA Instruments). The crystalline drug or mixture of NTR and polymer (5 mg) was melted at a temperature approximately 20 °C above its melting point and then cooled to approximately 100 °C below the T_g at a cooling rate of 40 °C/min. Thermal and photo degradation of the drugs was checked by HPLC, and no change in the chromatograms was observed after the preparation in comparison with that before. Fig. 2 shows typical DSC thermograms for the four amorphous drugs immediately after preparation and after subsequent storage. The T_g values for the amorphous drugs were: NLV, 48.6 ± 0.3 °C; NFD, 46.2 ± 0.2 °C; *m*-NFD, 41.3 ± 0.1 °C; NTR, 32.4 ± 0.3 °C. As shown in Fig. 2(b), freshly prepared amorphous NFD exhibited two endothermic peaks at around 161 °C and 168 °C. The two melting points of the peaks agreed well with that for the metastable form II and stable form I, respectively (Burger and Koller, 1996). As shown in Fig. 2(c), the NFD sample, retaining an amorphous portion after 5 h storage at 60 °C, showed exothermic peaks due to crystallization of the amorphous phase and its transformation into a stable crystal, and melted at 168 °C, which is approximately the same temperature as the melting point of the intact crystal. As shown in Fig. 2(d), the sample stored at 60 °C for 46 h showed the exothermic peak around 120–140 °C due to transformation into a stable crystal, although change in the heat capacity (ΔC_p) at T_g was not significant. The exothermic peak around 120–140 °C due to transformation into a stable crystal was also observed during storage at 50 °C and 70 °C (thermogram not shown). These DSC thermograms suggested that amorphous NFD initially crystallized into a metastable form. Crystallization into the metastable form was also observed during storage at 50 °C and 70 °C (thermogram not shown). Amorphous *m*-NFD showed an exothermic peak due to crystallization but no obvious peak due to transformation into a stable form like that shown by the NFD samples, and melted at 206 °C, which is approximately the same temperature as the melting point of intact *m*-NFD (Fig. 2(f) and (g)). It is not clear from the DSC thermograms whether transition to a stable or a metastable crystalline form occurred during storage. Fig. 2(j) and (k) show the DSC thermograms of the partially crystallized NTR samples showing one melting peak at 128 °C. The observed melting point was lower than that of the stable crystal

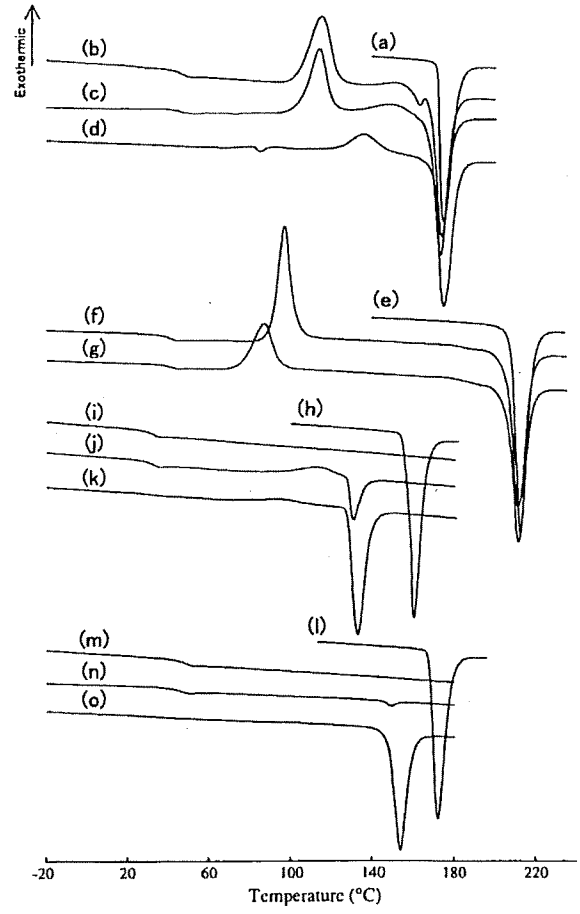

Fig. 2. Typical DSC thermograms: (a) NFD crystalline in the stable form, (b) freshly prepared amorphous NFD, (c) amorphous NFD after 5h-storage at 60 °C (d) amorphous NFD after 46 h-storage at 60 °C, (e) m-NFD crystalline in the stable form, (f) freshly prepared amorphous m-NFD, (g) amorphous m-NFD after 15 h-storage at 50 °C, (h) NTR crystalline in the stable form, (i) freshly prepared amorphous NTR, (j) amorphous NTR after 2 h-storage at 60 °C, (k) amorphous NTR after 9.75 h-storage at 60 °C, (l) NLV crystalline in the stable form, (m) freshly prepared amorphous NLV, (n) amorphous NLV after 48 h-storage at 80 °C, (o) amorphous NLV after 168 h-storage at 80 °C. Heating rate: 20 °C/min.

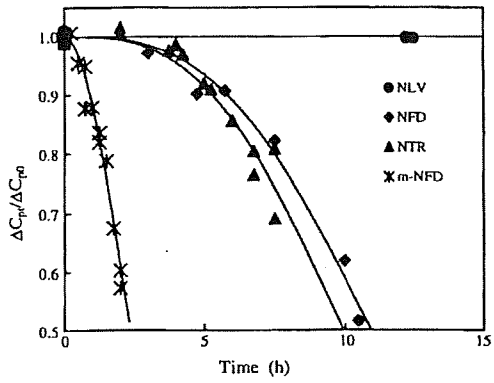

Fig. 3. Time profiles of crystallization for four dihydropyridines at 60 °C and 0%RH. The ratio of the amorphous form remaining at time t was calculated from the ΔC_p value assuming that the amount of amorphous phase is proportional to the ΔC_p. ΔC_{p0} and ΔC_{pt} are changes in ΔC_p at time 0 and t, respectively. Solid lines denote the fitting to the Avrami equation ($x(t) = \exp[-kt^n]$, $n = 3$).

Table 1
T_g values of amorphous NLV and NTR

RH (%)	T_g (°C)	
	NLV	NTR
0 (P_2O_5)	48.6 ± 0.3	32.4 ± 0.3
12 ($LiCl{\cdot}2H_2O$)	48.1 ± 0.7	30.5 ± 0.4
25 (CH_3COOK)	46.4 ± 0.5	29.0 ± 0.3
43 ($K_2CO_3{\cdot}2H_2O$)	43.4 ± 0.4	25.8 ± 0.3

For water absorption, the samples were kept at 5 °C for approximately 50 h in a desiccator containing saturated salt solutions. No crystallization was observed during the water absorption, as indicated by no endothermic melting peak in DSC thermograms.

(158 °C) and consistent with that reported for a metastable crystal (Kuhnert-Brandstätter and Völlenklee, 1986; Burger et al., 1997). As shown in Fig. 2(n) and (o), the partially crystallized NLV samples showed one melting peak at 148 °C. The observed melting point was lower than that for a stable crystal (168 °C) and similar to that for the dehydrated form of the monohydrate (Hirayama et al., 2000). Both amorphous NTR and NLV samples were considered to crystallize to their metastable crystalline forms under the conditions studied.

Fig. 3 shows the time profiles of crystallization of NFD, *m*-NFD, NTR, NLV at 60 °C and 0%RH. The crystallization rate was in the order: NLV < NTR = NFD < *m*-NFD. Fig. 4 shows the temperature dependence of the time required for 10% crystallization (t_{90}). Although NFD and NLV have approximately the same T_g, their values of t_{90} at the same temperature differed by more than two orders of magnitude (Fig. 4(A)). As shown in Fig. 4(B), the value of t_{90} at a given T_g/T (T being storage temperature) was in the order: NLV > NTR > NFD ≈ *m*-NFD within the whole range of temperature studied. As shown in Fig. 1, the four dihydropyridines have various alkyl groups at one of the carbonylester positions (R_2), and differ in the substitution position of the nitro group in the phenyl moiety (R_3 or R_4). The bulkiness of R_2 shows the order: NFD, *m*-NFD (methyl) < NTR (ethyl) < NLV (isopropyl). Furthermore, the substituent at R_1 is a cyano group in NLV, whereas it is a methyl group in the other three drugs; thus, the structural symmetry of NLV is lower. Since the plots for NFD and *m*-NFD in Fig. 4(B) almost overlapped each other, the difference in the crystallization rate may be attributed to the difference in molecular mobility. In contrast, differences in the crystallization rate between NLV, NTR and NFD cannot be explained only by the difference in molecular mobility. The differences in structural symmetry and bulkiness of functional group may cause differences in the Gibbs free energy and nucleus/amorphous interfacial energy, resulting in the differing crystallization rates between these drugs.

The crystallization rate of amorphous NLV and NTR solids with differing T_g values due to differing water content was measured to elucidate the effect of T_g on the crystallization rate (Table 1). The partially crystallized NLV and NTR in the presence of water showed an endothermic melting peak at approximately 150 °C and 130 °C, respectively. This suggests that amorphous NLV and NTR containing water also crystallize into their metastable forms in a similar manner as shown for dry samples. Fig. 5(A) shows the temperature dependence of the t_{90} obtained for NLV and NTR in the presence of water. When compared at the same temperature, the t_{90} value decreased with increasing RH. As shown in Fig. 5(B), the t_{90} versus T_g/T plots for each drug overlapped with those obtained under dry conditions, suggesting that the effect of water on the t_{90} value was explainable by the plasticizing effect of absorbed water,

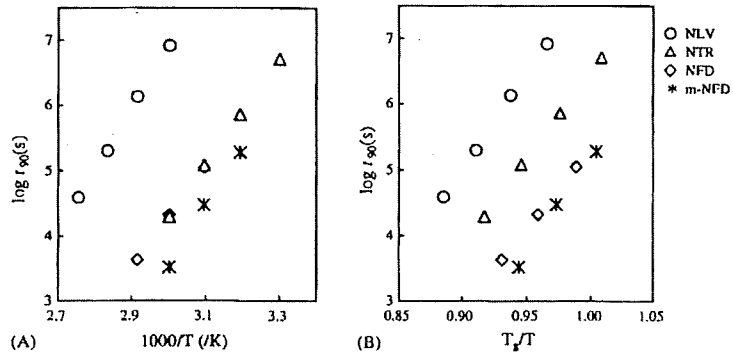

Fig. 4. Relationship between t_{90} for crystallization of drugs and storage temperature under dry conditions.

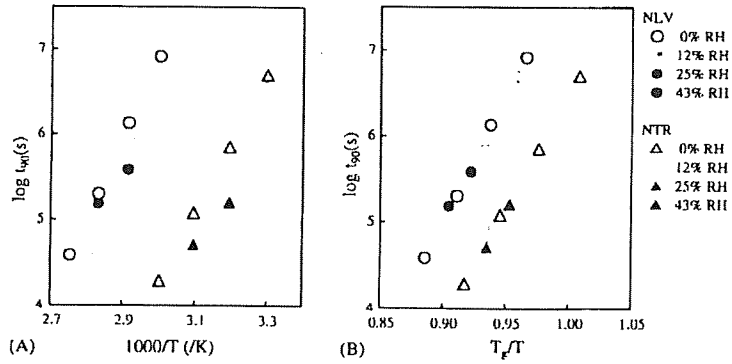

Fig. 5. Effect of absorbed water on the t_{90} of crystallization for NLV (circles) and NTR (triangles). The t_{90} values were measured at the early stage of crystallization at which no marked change in Tg was evident.

Table 2
T_g values of NTR-polymer solid dispersions

Polymer (%)	T_g (°C)	
	PVP	HPMC
0	32.4 ± 0.3	
3	33.2 ± 0.2	32.4 ± 0.1
5	34.1 ± 0.3	32.9 ± 0.4
6	34.1 ± 0.3	32.8 ± 0.2
11	36.6 ± 0.3	33.4 ± 0.3
20	–	33.7 ± 0.7
23	43.4 ± 0.8	–

similarly to that reported for NFD crystallization (Aso et al., 1995).

The effect of T_g on the crystallization rate of NTR was also investigated in solid dispersions with PVP and HPMC. A single T_g was observed for amorphous NTR-polymer solid dispersions prepared with 2.7–23% polymer excipients, indicating that NTR and polymer are miscible within the sensitivity limit of the DSC method. The value of T_g tended to increase with the amount of polymer, and the extent of increase was greater for NTR-PVP dispersions than for NTR-HPMC dispersions (Table 2). As the partially crystallized NTR-polymer dispersions showed a melt-

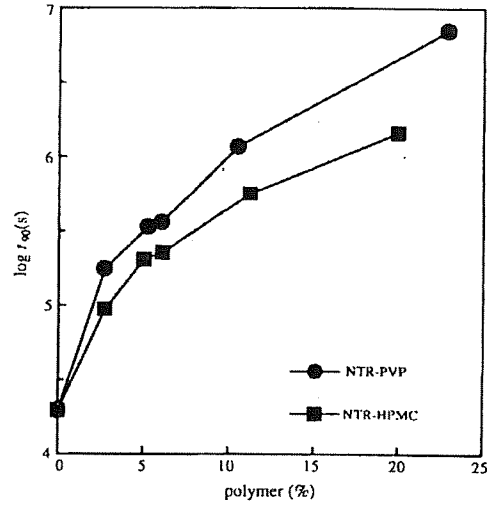

Fig. 6. Effect of polymer content on crystallization of NTR in solid dispersions with PVP and HPMC at 60 °C and 0%RH.

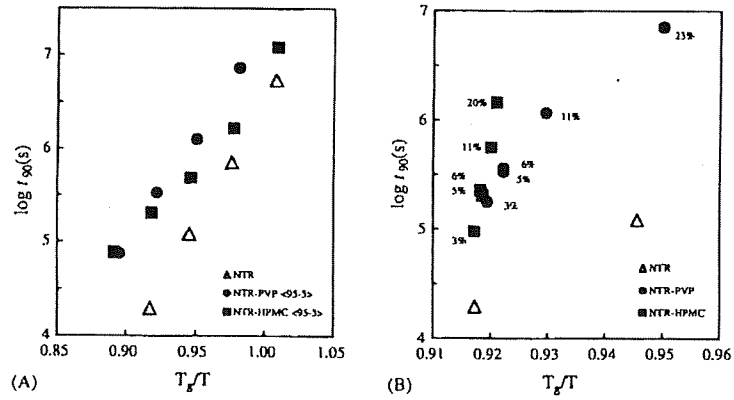

Fig. 7. Relationship between T_g/T and t_{90} of crystallization for NTR in the pure amorphous form and solid dispersions with PVP and HPMC. Numbers in percentage terms in figure (B) denote polymer contents.

ing peak at approximately 130 °C, the crystallization of NTR in the presence of the polymers was considered to be transition into a metastable form in a similar manner as that observed for pure amorphous NTR. Fig. 6 shows the effect of polymer excipients on the t_{90} values. Both PVP and HPMC increased t_{90} as the amount of polymer increased, but PVP was more effective in stabilizing amorphous NTR within the range of content studied. Fig. 7(A) shows the temperature dependence of t_{90} for solid dispersions containing 5% polymer. The t_{90} value compared at the same T_g/T was longer for both NTR-polymer dispersions than for pure NTR. Furthermore, the t_{90} versus T_g/T plots for solid dispersions containing various amounts of polymers did not overlap with that for pure NTR (Fig. 7(B)), indicating that crystallization of NTR was inhibited by the addition of PVP and HPMC to a greater extent than expected from the increased T_g. The present results imply that the drug-polymer interaction as well as an antiplasticizing effect of polymer excipients retarded the crystallization of the amorphous solid (Hirasawa et al., 2003a,b, 2004; Aso et al., 2004; Miyazaki et al., 2004, 2006; Wang et al., 2006).

Acknowledgement

A part of this work was supported by a grant from the Japan Health Science Foundation.

References

Andronis, V., Zografi, G., 2000. Crystal nucleation and growth of indomethacin polymorphs from the amorphous state. J. Non-Cryst. Solids 271, 236–248.

Aso, Y., Yoshioka, S., Otsuka, T., Kojima, S., 1995. The physical stability of amorphous nifedipine determined by isothermal microcalorimetry. Chem. Pharm. Bull. 43, 300–303.

Aso, Y., Yoshioka, S., Kojima, S., 2001. Explanation of the crystallization rate of amorphous nifedipine and Phenobarbital from their molecular mobility as measured by ^{13}C nuclear magnetic resonance relaxation time and the relaxation time obtained from the heating rate dependence of the glass transition temperature. J. Pharm. Sci. 90, 798–806.

Aso, Y., Yoshioka, S., Kojima, S., 2004. Molecular mobility-based estimation of the crystallization rates of amorphous nifedipine and Phenobarbital in poly(vinylpyrrolidone) solid dispersions. J. Pharm. Sci. 93, 384–391.

Burger, A., Koller, K.T., 1996. Polymorphism and pseudopolymorphism on nifedipine. Sci. Pharm. 64, 293–301.

Burger, A., Rollinger, J.M., Brüggeller, P., 1997. Binary system of (*R*)- and (*S*)-nitrendipine—polymorphism and structure. J. Pharm. Sci. 86, 674–679.

Hancock, B.C., Zografi, G., 1997. Characteristics and significance of the amorphous state in pharmaceutical systems. J. Pharm. Sci. 86, 1–12.

Hirasawa, N., Ishise, S., Miyata, H., Danjo, K., 2003a. Physicochemical characterization and drug release studies of Nilvadipine solid dispersions using water-insoluble polymer as a carrier. Drug Dev. Ind. Pharm. 29, 339–344.

Hirasawa, N., Ishise, S., Miyata, H., Danjo, K., 2003b. An attempt to stabilize Nilvadipine solid dispersion by the use of ternary systems. Drug Dev. Ind. Pharm. 29, 997–1004.

Hirasawa, N., Ishise, S., Miyata, H., Danjo, K., 2004. Application of Nilvadipine solid dispersion to tablet formulation and manufacturing using crospovidone and methylcellulose as dispersion carriers. Chem. Pharm. Bull. 52, 244–247.

Hirayama, F., Honjo, M., Arima, H., Okimoto, K., Uekama, K., 2000. X-ray crystallographic characterization of Nilvadipine monohydrate and its phase transition behavior. Eur. J. Pharm. Sci. 11, 81–88.

Kuhnert-Brandstätter, M., Völlenklee, R., 1986. Beitrag zur polymorphie von arzneistoffen 2. Mitteilung: halofenat, lorcainidhydrochlorid, minoxidil, mopidamol und nitrendipin. Sci. Pharm. 54, 71–82.

Miyazaki, T., Yoshioka, S., Aso, Y., Kojima, S., 2004. Ability of polyvinylpyrrolidone and polyacrylic acid to inhibit the crystallization of amorphous acetaminophen. J. Pharm. Sci. 93, 2710–2717.

Miyazaki, T., Yoshioka, S., Aso, Y., 2006. Physical stability of amorphous acetanilide derivatives improved by polymer excipients. Chem. Pharm. Bull. 54, 1207–1210.

Ngai, K.L., Magill, J.H., Plazek, D.J., 2000. Flow, diffusion and crystallization of supercooled liquids: revisited. J. Chem. Phys. 112, 1887–1892.

Rodríguez-Hornedo, N., Murphy, D., 1999. Significance of controlling crystallization mechanisms and kinetics in pharmaceutical systems. J. Pharm. Sci. 88, 651–660.

Saleki-Gerhardt, A., Zografi, G., 1994. Non-isothermal and isothermal crystallization of sucrose from the amorphous state. Pharm. Res. 11, 1166–1173.

Wang, L., Cui, F.D., Hayase, T., Sunada, H., 2005. Preparation and evaluation of solid dispersion for Nitrendipine-carbopol and Nitrendipine-HPMCP systems using a twin screw extruder. Chem. Pharm. Bull. 53, 1240–1245.

Wang, L., Cui, F.D., Sunada, H., 2006. Preparation and evaluation of solid dispersions of Nitrendipine prepared with fine silica particles using the melt-mixing method. Chem. Pharm. Bull. 54, 37–43.

Zhou, D., Zhang, G.G.Z., Law, D., Grant, K.J.W., Schmitt, E.A., 2002. Physical stability of amorphous pharmaceuticals: importance of configurational thermodynamic quantities and molecular mobility. J. Pharm. Sci. 91, 1863–1872.

Miscibility of Nifedipine and Hydrophilic Polymers as Measured by ^{1}H-NMR Spin–Lattice Relaxation

Yukio Aso,*[a] Sumie Yoshioka,[a] Tamaki Miyazaki,[a] Tohru Kawanishi,[a] Kazuyuki Tanaka,[b] Satoshi Kitamura,[b] Asako Takakura,[c] Takashi Hayashi,[c] and Noriyuki Muranushi[c]

[a] *National Institute of Health Sciences; 1–18–1 Kamiyoga, Setagaya-ku, Tokyo 158–8501, Japan:* [b] *Astellas Pharma Inc.; 180 Ozumi, Yaizu, Shizuoka 425–0072, Japan: and* [c] *Shionogi & Co., Ltd.; 2–1–3 Kuise, Terajima, Amagasaki, Hyogo 660–0813, Japan.* Received April 19, 2007; accepted June 4, 2007; published online June 5, 2007

The miscibility of a drug with excipients in solid dispersions is considered to be one of the most important factors for preparation of stable amorphous solid dispersions. The purpose of the present study was to elucidate the feasibility of ^{1}H-NMR spin–lattice relaxation measurements to assess the miscibility of a drug with excipients. Solid dispersions of nifedipine with the hydrophilic polymers poly(vinylpyrrolidone) (PVP), hydroxypropylmethylcellulose (HPMC) and α,β-poly(*N*-5-hydroxypentyl)-L-aspartamide (PHPA) with various weight ratios were prepared by spray drying, and the spin–lattice relaxation decay of the solid dispersions in a laboratory frame (T_1 decay) and in a rotating frame ($T_{1\rho}$ decay) were measured. $T_{1\rho}$ decay of nifedipine–PVP solid dispersions (3 : 7, 5 : 5 and 7 : 3) was describable with a mono-exponential equation, whereas $T_{1\rho}$ decay of nifedipine–PHPA solid dispersions (3 : 7, 4 : 6 and 5 : 5) was describable with a bi-exponential equation. Because a mono-exponential $T_{1\rho}$ decay indicates that the domain sizes of nifedipine and polymer in solid dispersion are less than several nm, it is speculated that nifedipine is miscible with PVP but not miscible with PHPA. All the nifedipine–PVP solid dispersions studied showed a single glass transition temperature (T_g), whereas two glass transitions were observed for the nifedipine–PHPA solid dispersion (3 : 7), thus supporting the above speculation. For nifedipine–HPMC solid dispersions (3 : 7 and 5 : 5), the miscibility of nifedipine and HPMC could not be determined by DSC measurements due to the lack of obviously evident T_g. In contrast, ^{1}H-NMR spin–lattice relaxation measurements showed that nifedipine and HPMC are miscible, since $T_{1\rho}$ decay of the solid dispersions (3 : 7, 5 : 5 and 7 : 3) was describable with a mono-exponential equation. These results indicate that ^{1}H-NMR spin–lattice relaxation measurements are useful for assessing the miscibility of a drug and an excipient in solid dispersions.

Key words miscibility; solid dispersion; spin diffusion; spin–lattice relaxation time; amorphous

Preparing solid dispersions of a poorly soluble drug with water-soluble polymers is a promising method for improving the dissolution characteristics and bioavailability of the drug. Miscibility between a drug and a polymer is considered to be one of the most important factors for obtaining stable solid dispersions.[1)]

Miscibility of a drug with a polymer is usually evaluated by differential scanning calorimetry (DSC).[2—6)] When a solid dispersion shows a single glass transition temperature (T_g) between the T_g values of the drug and the polymer, the drug and the polymer are considered to be miscible within the detection limit of DSC.[7)] This method is applicable to a solid dispersion when T_g of the drug and the polymer can be detected clearly, and the temperature ranges of the base line shift due to glass transition do not overlap each other.

The interaction parameter χ of the Flory–Huggins equation provides a measure of miscibility.[8,9)] Crowly and Zografi measured the water vapor sorption isotherm of indomethacin solid dispersions with PVP and reported that the estimated interaction parameter χ between indomethacin and PVP was greater than 0.5, indicating that indomethacin and PVP are immiscible in terms of χ value.[8)] Although this method is excellent in being able to provide a quantitative measure of miscibility, it may be difficult to apply to unstable amorphous drugs, which crystallize during measurement of water vapor sorption.

A method that can be used as an alternative to DSC or measurement of the interaction parameter χ is analysis of the ^{1}H spin–lattice relaxation process of solid dispersions, which has been reported in the fields of polymer alloy and polymer blends. If two polymers are miscible, the relaxation decay of the mixture is describable by a mono-exponential equation, whereas if they are not miscible, relaxation decay is describable by a bi-exponential equation.[10,11)]

In this paper, the feasibility of ^{1}H spin–lattice relaxation measurements for evaluating the miscibility of a drug and polymers in solid dispersions was studied. Nifedipine solid dispersions with PVP, HPMC and α,β-poly(*N*-5-hydroxypentyl)-L-aspartamide (PHPA) were used as model solid dispersions, and the miscibility measured by ^{1}H-NMR was compared with that measured by DSC. The dissolution profiles of nifedipine from PVP solid dispersions were compared with those from PHPA solid dispersions to discuss the effects of miscibility on the dissolution rate of nifedipine.

Theory ^{1}H spin–lattice relaxation rates of respective spins in a solid are usually averaged by a process called spin diffusion. Spin diffusion is the equilibration process of polarizations of spins at different local sites through mutual exchange of magnetization. ^{1}H spin–lattice relaxation decay for a single-phase solid is describable by a mono-exponential equation with a relaxation rate that is averaged by spin diffusion. When a solid consists of two phases, the spin–lattice relaxation decay is describable by a mono-exponential or a bi-exponential equation depending on both the domain size of each phase and the effective diffusion length (L). L is expressed as follows:

$$L=\sqrt{6Dt} \quad (1)$$

* To whom correspondence should be addressed. e-mail: aso@nihs.go.jp

where D is the spin diffusion coefficient, and t is the diffusion time. D is a function of the distance between neighboring proton spins and spin–spin relaxation time (T_2), and is reported to be approximately 10^{-12} cm^2 s^{-1} for organic polymers. Typical spin–lattice relaxation time in a laboratory frame (T_1) and that in a rotating frame ($T_{1\rho}$) are of the order of 1 s and 10 ms, respectively. When these values for t were inserted in Eq. 1, effective diffusion lengths of approximately 50 nm and 5 nm were obtained for T_1 and $T_{1\rho}$, respectively. Depending on the domain size of each phase in a solid, the following 3 cases can be expected: (1) when the domain is smaller than about 5 nm, both the spin–lattice relaxation decay patterns in a laboratory frame (T_1 decay) and in a rotating frame ($T_{1\rho}$ decay) are describable by a mono-exponential equation; (2) when the domain size is about 5 to 50 nm, the $T_{1\rho}$ decay pattern is describable by a bi-exponential equation, whereas the T_1 decay pattern is describable by a mono-exponential equation; and (3) when the domain size is larger than about 50 nm, both the T_1 and $T_{1\rho}$ decay patterns are describable by a bi-exponential equation. When the $T_{1\rho}$ decay is describable by a mono-exponential equation, the solid can be considered as a single phase within the detection limit of NMR. T_1 and $T_{1\rho}$ decay thus provide information on miscibility of a drug and a polymer excipient.[11]

Experimental

Materials Nifedipine (N-7634), PVP (PVP-40) and HPMC (H-3785) were purchased from Sigma (Newcastle, DE, U.S.A.). PHPA was synthesized *via* polycondensation of L-aspartic acid.[12] Phenobarbital was obtained from sodium phenobarbital (Wako Pure Chemical Ind., Osaka) by neutralization and subsequent re-crystallization from acetone solutions as described previously.[13] Other chemicals used were of reagent grade. Nifedipine solid dispersions with PVP, HPMC and PHPA were prepared by a solvent evaporation method using a model GS-310 spray dryer (Yamato, Tokyo, Japan). Drying conditions are summarized in Table 1. The solid dispersions obtained were confirmed to be amorphous from microscopic observation under polarized light. Although the drying conditions were not optimized, 50 to 90% of the solid dispersions were obtained. Amorphous nifedipine was prepared by melting and subsequent rapid cooling as reported previously.[14]

DSC T_g of nifedipine–PVP and nifedipine–HPMC solid dispersions was measured by modulated temperature DSC using a model 2920 differential scanning calorimeter and a refrigerator cooling system (TA Instruments, Newcastle, DE, U.S.A.). The modulated temperature program used was a modulation amplitude of ±0.5 °C, a modulation period of 100 s and an underlying heating rate of 1 °C/min. For nifedipine–PHPA solid dispersions, T_g was measured at a scanning rate of 20 °C/min using a conventional heating program. Temperature calibration of the instrument was carried out using indium.

NMR T_1 decay and $T_{1\rho}$ decay were measured using a model JNM-MU25 pulsed NMR spectrometer (JEOL DATUM, Tokyo, Japan). The inversion recovery pulse sequence was used to measure T_1 decay. $T_{1\rho}$ decay was measured in a spin locking field of 10 G. All measurements were carried out at 27 °C.

X-Ray Powder Diffraction X-Ray powder diffraction patterns of solid dispersions were obtained using a model RINT-TTR II X-ray diffractometer (Rigaku Denki, Tokyo) with Cu$K\alpha$ radiation (50 kV, 300 mA) at a scanning rate of 4 °C/min from 2θ=5° to 40°.

Nifedipine Dissolution Profile Nifedipine–PVP (3 : 7) and nifedipine–PHPA (3 : 7) solid dispersions containing 100 mg of nifedipine were made into disks with a diameter of 2 cm at a pressure of 20 kN. Each disk was mounted on the rotor of the dissolution apparatus and the side surface of the disk was covered with a Teflon film. The sample was rotated at a rate of 100 rpm in 900 ml of distilled water at 37 °C. The amount of nifedipine dissolved was measured using a model DM-3100 solution monitor (Otsuka Electronics, Tokyo).

Results and Discussion

Figure 1 shows typical T_1 and $T_{1\rho}$ decay patterns for the solid dispersion and the physical mixture of nifedipine and PHPA (3 : 7). T_1 and $T_{1\rho}$ decay patterns were mono-exponential for both amorphous nifedipine and PHPA. The T_1 and $T_{1\rho}$ values of nifedipine were 5.0 s and 104 ms, respectively, and those of PHPA were 0.084 s and 4.4 ms, respectively. The physical mixture of nifedipine and PHPA (3 : 7) exhibited bi-exponential T_1 and $T_{1\rho}$ decay with the relaxation time of each component, indicating that the particle sizes of nifedipine and PHPA in the physical mixture are much larger than the effective diffusion length (approximately 5 nm and 50 nm for $T_{1\rho}$ and T_1 decay, respectively). In contrast to the physical

Table 1. Conditions of Spray Drying

Drug	Polymer	Solvent[a]	Outlet temperature (°C)	Atomizer gas (l/min)	Feeding rate (ml/min)
Nifedipine–PHPA					
0	10	A	68	7	5
3	7	A	68	7	3
4	6	A	68	7	3
5	5	A	68	7	3
Phenobarbital–PHPA					
3	7	A	68	7	3
Nifedipine–PVP					
0	10	A	90	9	10
3	7	A	90	9	10
5	5	A	90	9	10
7	3	A	68	7	3
Nifedipine–HPMC					
0	10	B	38	11	3
3	7	B	38	11	2
5	5	B	38	11	2
7	3	B	38	11	4

a) Solvent A, ethanol; solvent B, ethanol–CH_2Cl_2 (1 : 1). Flow rate of drying gas was adjusted to 0.5 m^3/min.

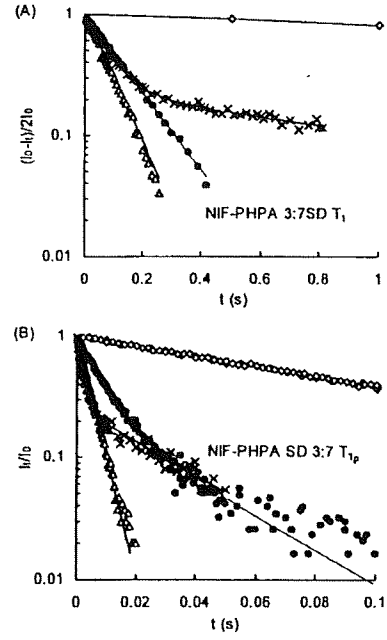

Fig. 1. T_1 (A) and $T_{1\rho}$ (B) Decay Patterns for Amorphous Nifedipine (◇), Amorphous PHPA (△), Physical Mixture (×) and Solid Dispersions (●) of Nifedipine and PHPA

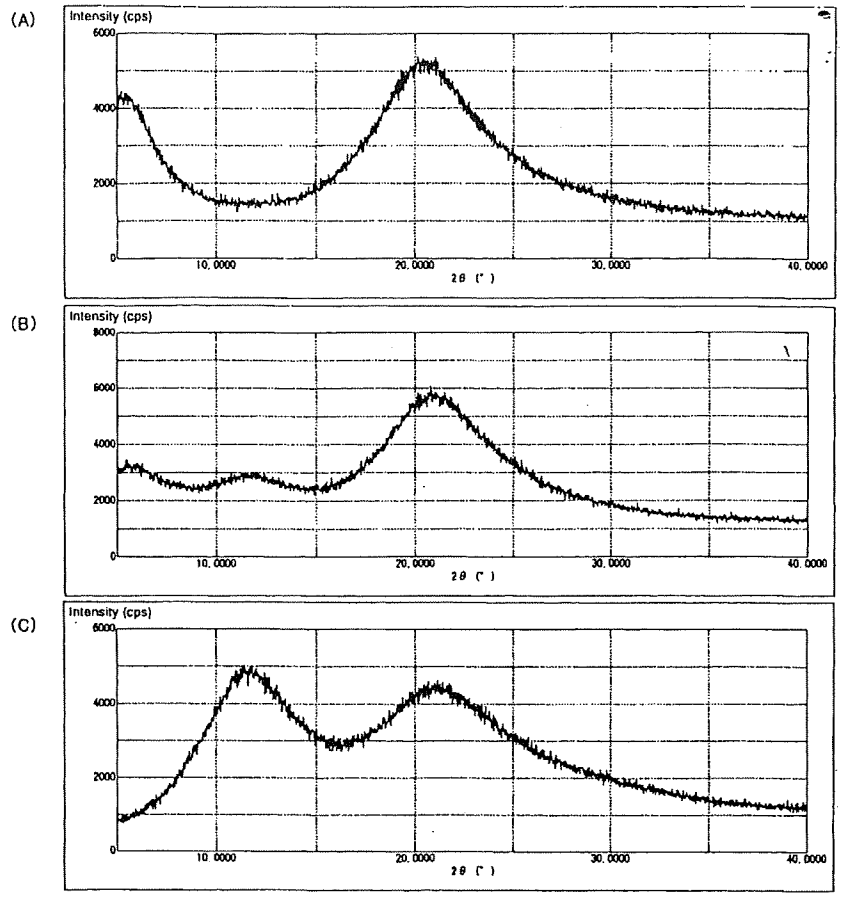

Fig. 2. Powder X-Ray Diffraction Patterns of PHPA (A), Nifedipine–PHPA (3 : 7) (B) and Nifedipine–PVP Solid Dispersions (3 : 7) (C)

mixture, the solid dispersion (3 : 7) showed mono-exponential T_1 decay, whereas bi-exponential $T_{1\rho}$ decay. These results indicate that nifedipine and PHPA are immiscible and that domains 5 to 50 nm in size are present in the solid dispersion. The nifedipine–PHPA solid dispersions (4 : 6 and 5 : 5) and the phenobarbital–PHPA solid dispersions (3 : 7) also exhibited bi-exponential $T_{1\rho}$ decay (data not shown). Figure 2 shows powder X-ray diffraction patterns of the nifedipine–PHPA and nifedipine–PVP solid dispersions. The observed halo pattern indicates that nifedipine in the PHPA dispersions is amorphous at the detection limit of powder X-ray diffractometry.

DSC data supported the contention that nifedipine and PHPA are immiscible. Figure 3 shows typical DSC traces for nifedipine–PHPA solid dispersions. The nifedipine–PHPA solid dispersion (3 : 7) showed glass transition at approximately 50 °C, corresponding to the T_g of amorphous nifedipine, and at approximately 75 °C, indicating that there are both an amorphous nifedipine phase and an amorphous nifedipine–PHPA phase in the solid dispersion. These DSC data indicate that amorphous nifedipine and PHPA are partially immiscible at this weight ratio. For the nifedipine–PHPA solid dispersion (5 : 5), T_g of the amorphous nifedipine–PHPA phase was not clearly observed because of the detection limit of DSC, suggesting that ^{1}H-NMR relaxation measurements can detect immiscibility of drugs and polymers more sensitively than DSC. DSC data suggest that the nifedipine–PHPA solid dispersion (3 : 7) consists of pure amorphous nifedipine phase and amorphous nifedipine–PHPA phase. NMR data may support this speculation. As shown in Fig. 1B, initial $T_{1\rho}$ decay of the solid dispersion was slower than that of the physical mixture or pure PHPA. This slow relaxation rate of the solid dispersion may indicate that the relaxation rate of PHPA protons was decreased by spin diffusion with nifedipine protons existing near PHPA molecules; in other words, nifedipine–PHPA phase is considered to exist in the solid dispersion. The effect of weight ratios on the $T_{1\rho}$ decay of nifedipine–PHPA solid dispersions needs to examine in order

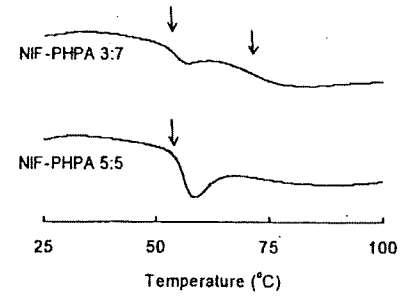

Fig. 3. DSC Traces for Nifedipine–PHPA Solid Dispersions
Arrows represent T_g.

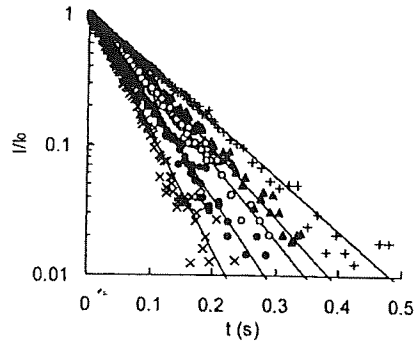

Fig. 4. $T_{1\rho}$ Decay Patterns for Nifedipine (+), PVP (×), and Nifedipine–PVP Solid Dispersions of 7 : 3 (▲), 5 : 5 (○), and 3 : 7 (●)

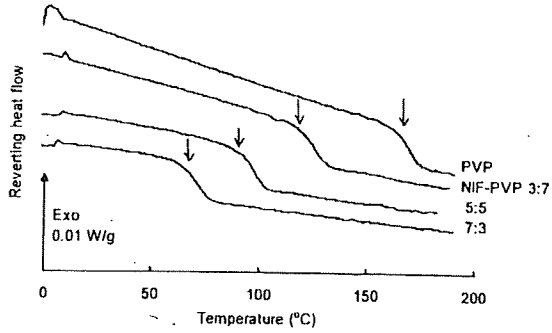

Fig. 5. DSC Traces for Nifedipine–PVP Solid Dispersions
Arrows represent T_g.

to confirm the phase structure of the solid dispersion, since the molecular mobility of PHPA may different from that of pure PHPA.

In contrast to PHPA, PVP and nifedipine in the solid dispersions (3 : 7, 5 : 5 and 7 : 3) were considered to be miscible from $T_{1\rho}$ relaxation and DSC measurements. Figure 4 shows typical $T_{1\rho}$ decay of the solid dispersions. All the solid dispersions studied exhibited mono-exponential $T_{1\rho}$ decay, whereas physical mixtures of amorphous nifedipine and PVP (3 : 7, 5 : 5 and 7 : 3) exhibited bi-exponential decay (data not shown). Figure 5 shows DSC traces for the nifedipine–PVP solid dispersions. A single glass transition was observed for all of the solid dispersions studied. These data indicate that nifedipine and PVP are miscible at the detection limit of NMR and DSC.

For nifedipine–HPMC solid dispersions, the miscibility of nifedipine and HPMC could not be assessed from T_g measurements. As shown in Fig. 6, base line shift due to glass transition was not obvious for the nifedipine–HPMC solid dispersions (3 : 7 and 5 : 5). In contrast to DSC measurements, $T_{1\rho}$ relaxation measurements clearly indicated that nifedipine is miscible with HPMC in the solid dispersions. As shown in Fig. 7, all the nifedipine–HPMC solid dispersions studied showed mono-exponential $T_{1\rho}$ decay. In contrast to the solid dispersions, physical mixtures of amorphous nifedipine and HPMC (3 : 7, 5 : 5 and 7 : 3) exhibited bi-exponential decay (data not shown). These data indicate that NMR can detect miscibility of a drug and an excipient more sensitively than DSC.

Figure 8 shows the dissolution profile of nifedipine from

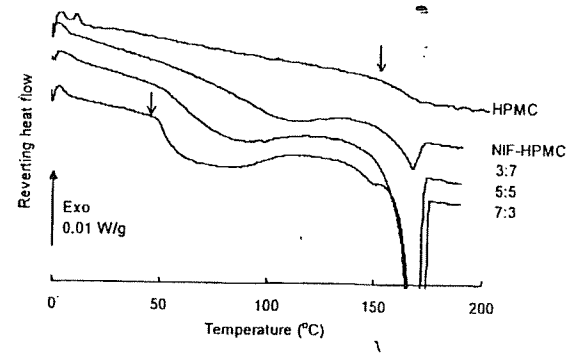

Fig. 6. DSC Traces for Nifedipine–HPMC Solid Dispersions
Arrows represent T_g.

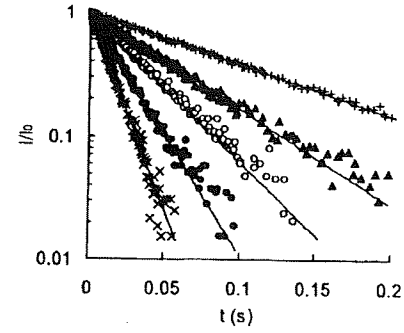

Fig. 7. $T_{1\rho}$ Decay Patterns for Nifedipine (+), HPMC (×), and Nifedipine–HPMC Solid Dispersions of 7 : 3 (▲), 5 : 5 (○), and 3 : 7 (●)

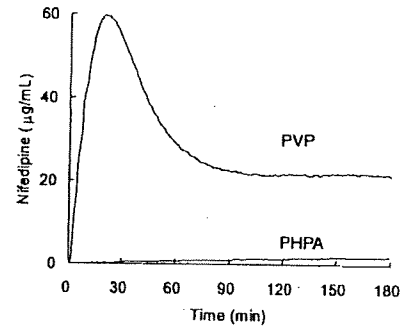

Fig. 8. Dissolution Profiles of Nifedipine from Solid Dispersions with PVP and PHPA

solid dispersions with PVP and PHPA. The nifedipine–PVP solid dispersion exhibited rapid dissolition of nifedipine with super-saturation. In contrast, only a minimal amount of nifedipine was dissolved from the nifedipine–PHPA solid dispersion.

In conclusion, ^{1}H- NMR spin–lattice relaxation measurements were found to be useful for assessing the miscibility of a drug and excipients in solid dispersions, especially, when T_g is not clearly detected by DSC. The lower miscibility of PHPA than that of PVP and HPMC with hydrophobic drugs is considered due to the more hydrophilic nature of PHPA.

Acknowledgements A part of this work was supported by a Grant-in-aid for Research on Publicly Essential Drugs and Medical Devices from The Japan Health Sciences Foundation.

References

1) Forster A., Hempenstall J., Tucker I., Rades T., *Int. J. Pharm.*, **226**, 147—161 (2001).
2) Lu Q., Zografi G., *Pharm. Res.*, **15**, 1202—1206 (1998).
3) Khougaz K., Clas S. D., *J. Pharm. Sci.*, **89**, 1325—1334 (2000).
4) Tong P., Zografi G., *J. Pharm. Sci.*, **90**, 1991—2004 (2001).
5) Vasanthavada M., Tong W. Q., Joshi Y., Kislalioglu M. S., *Pharm. Res.*, **21**, 1598—1606 (2004).
6) Shmeis R. A., Wang Z., Krill S. L., *Pharm. Res.*, **21**, 2025—2030 (2004).
7) Kaplan D. S., *J. Appl. Polym. Sci.*, **20**, 2615—2629 (1976).
8) Crowly K. J., Zografi G., *J. Pharm. Sci.*, **91**, 2150—2165 (2002).
9) Marsac P. J., Shamblin S. L., Taylor L. S., *Pharm. Res.*, **23**, 2417—2426 (2006).
10) Cheung M. K., *Polymer*, **41**, 1469—1474 (2000).
11) Asano A., Takegoshi K., "Solid State NMR of Polymers," Chap. 10, ed. by Ando I., Asakura T., Elsevier, Amsterdam, 1998, pp. 351—414.
12) Giammona G., Carlisi B., Plazzo S., *J. Polym. Sci. Polym. Chem. Ed.*, **25**, 2813—2818 (1987).
13) Kato Y., Watanabe F., *Yakugaku Zasshi*, **98**, 639—648 (1978).
14) Aso Y., Yoshioka S., Kojima S., *J. Pharm. Sci.*, **89**, 408—416 (2000).

——資　　料——

医薬品研究
Pharm. Regul. Sci.
38(8)381～390(2007)

平成17年度「日本薬局方の試験法に関する研究」研究報告**

―バイオ医薬品の日局収載環境の整備に関する研究―

川　西　　徹*

目　　的

バイオ医薬品（細胞培養医薬品及び遺伝子組換え医薬品）の日局各条への収載は，14局におけるヒトインスリン（遺伝子組換え）に始まり，15局では更に3品目（セルモロイキン（遺伝子組換え），テセロイキン（遺伝子組換え），注射用テセロイキン（遺伝子組換え））が収載され，更に近々に収載が予定される品目は10品目以上にのぼる．しかし，今後バイオ医薬品の各条収載を円滑に進める上で，検討すべき課題が浮かび上がっている．その一つは，原案作成要領の整備である．現在収載案の作成にあたって参照している「15局作成要領」は，主として化学医薬品の収載案作成を目的としたものである．そのため，バイオ医薬品の各条収載案の作成ガイドとしては不十分な部分があり，長時間の各条審議が必要とされる原因の一つとなっている．したがって，早急に「バイオ医薬品の日局収載にあたっての作成要領」を整備することが望まれる．

そこで本研究は15局局方収載生物薬品原案作成にあたった担当会社の担当者を対象に，15局作成要領の問題点を調査し，15局作成要領の修正・追加が必要と考えられるポイントをまとめるとともに，その対応案を検討した．

研究方法

15局局方収載生物薬品の原案作成にあたった9社の作成担当者を対象に，15局原案作成要領の生物薬品に関連した部分において，問題点，わかりにくかった点，補うべき点等について，意見を収集した．これらの指摘をまとめるとともに，16局原案作成要領作成にあたって，改訂すべき点をまとめ，考察した．

研究結果及び考察

1.　指摘された問題点

回答は，6社の担当者から得ることができた．以下がそのまとめである．

1.1　構造式について

既収載の生物薬品の中には，純度が低いもの，あるいは有効成分が混合物からなるものが少なくなかった．しかし今後収載が予定されるバイオ医薬品のほとんどは，純度は極めて高く，有効成分の物理化学的性質，化学構造等の特性解析は相当程度になされており，構造情報の記載が求められる．しかし多様な物質が対象となるとともに，分子多様性を示す製品も多いため，従来作成要領には，その記載法は明確に示されていなかった．この点について，3社からの指摘があり，特に構造式及び分子式・分子量の記載方法を明記するようにという要望，N末，C末などに多様性を有するたん白質の場合の表記法の検討，糖たん白質の分子量の表記法に関する記載法の規準，糖鎖構造の表記法に関する意見が寄せられた．

1.2　基原・本質について

生物薬品においては，原薬においても化学構造式からその本質を表現することが困難なものが多かった．このようなものについては，基原，本質及び薬理作用を記載することによって医薬品を定義してきた．しかし医薬品の種類が多種，多様にわたるため，

* 国立医薬品食品衛生研究所　東京都世田谷区上用賀1-18-1（〒158-8501）

** 本研究は，平成17年度日本公定書協会の「日本薬局方の試験法に関する研究」により行ったものである．

基原，本質の記載法については明確にされていなかった．この点に，2社からの指摘があり，その記載法を例示するように要望が出された．

1.3　含量規格について

生物薬品ではバイオアッセイを用いる場合も多く，少数第一位までの%表記は困難という指摘がなされた．

1.4　試験法について

1.4.1　試験法の記載の簡略化

たん白質性医薬品の一般試験法として14局第1追補においてSDSポリアクリルアミド電気泳動法(SDS-PAGE法)，14局第2追補においてたん白質定量法，アミノ酸分析法，ペプチドマップ法，等電点電気泳動法，キャピラリー電気泳動法が収載された．これに伴い，たん白質定量法，SDS-PAGE法，アミノ酸分析法，ペプチドマップ法，等電点電気泳動法については簡略した記載でも可とするよう，要望が出された．

その他，ウェスタンブロット法などのたん白質分析に一般的に使用される試験の場合，あるいはバイオアッセイ法，ELISA法の場合のように検量線について多次回帰，4-パラメータなどで解析方法が非常に複雑な場合については，簡略な記載でも可とするような要望が出された．

また分析機器に依存するところが大きい，アミノ酸分析計，気相シーケンサー，糖鎖電気化学検出器等では，詳細な分析条件を記載するのではなく，機器の機能を特定するような記載（例えば，アミノ酸分析計における各種アミノ酸の分離度等）でも可とするよう要望が出された．

1.4.2　生物薬品特有の試験法の記載例の例示

各種電気泳動法，アミノ酸分析法，ペプチドマップ法，糖鎖マップ法などについては，記載例の作成の要望が出された．

1.4.3　製造工程由来不純物等の記載法

特にバイオ医薬品については，製造方法が異なると不純物が相当程度異なることから，製造工程由来不純物については各条試験法で一律に規定せず，製品に応じて承認申請時に個別に審査する方法が合理的と考えられる項目が少なくない．また各条に規定される規格試験によるのではなく，工程管理試験によってコントロールする方が品質管理法として合理的な場合も少なくない．このようなケースを想定して，15局通則11において「医薬品各条において「別に規定する」とあるのは，薬事法に基づく承認の際に規定することを示す」となっており，「別に規定する」として規格試験法や規格を各条に規定する必要はないとされてきた．しかし，その規準が明確でないので，特に純度試験関係で，宿主細胞や異種たん白質の設定の要否，具体的に規定すべきもの，「別に規定する」でよいもの等に関し，考え方を明記するように要望が出された．

1.4.4　平行線検定・力価

生物薬品の力価については“平行線検定”を行うべきものが多いが，“平行線検定”が日局では定義されていないため，これらの計算方法について詳細に備考に記載する必要が生じている．そこでEP/USPと同様に“平行線検定”を定義してほしいという要望が出された．

1.5　生物薬品と化学薬品との規格設定の違いについて

生物薬品においては原薬にエンドトキシンを設定する場合があるが，その場合，日局参考情報の他に実測値も考慮して設定すべきとされてきた．この点を明記するように要望が出された．

1.6　試薬・試液

生物薬品の試験に特有の試薬（血清・酵素・抗体等）の記述範囲について明確にできないか，あるいは試験に用いるキット製品について，記載案（どこまで略記するか）を作成要領に明確にするよう，3社から要望が出された．

2.　作成要領の改訂に関する検討，考察

2.1　構造式の表記について

15局で収載された品目の各条においては，ペプチド及びたん白質性医薬品のアミノ酸配列については，3文字法を採用してきた．今後収載される構造の複雑なたん白質も考慮し，3文字法（概ね20アミノ酸残基以下）以外にも，1文字法（概ね21アミノ酸残基以上）の表記も可とすることが適当と考えられた．更に，構造式の表記法について，ペプチド性医薬品，ペプチド性医薬品及びたん白質性医薬品（ヘテロダーマー），ペプチド性医薬品及びたん白質性医薬品（ホモダイマー），糖たん白質性医薬品にわけて例示することが適当と考えられた．

分子式及び分子量については，糖たん白質性医薬

品はたん白質部分の分子量・分子式のみを記載し，糖鎖を含めた分子量（概数）は基原に記載することが適当と考えられた．更に，ペプチド性医薬品，ペプチド性及びたん白質性医薬品，糖たん白質性医薬品に分けて，記載例を示すことが適当と考えられた．

2.2　基原・本質について

たん白質性医薬品の有効成分については，化学構造式のみでは本質が表現できないものが少なくない．更に糖たん白質のように翻訳後修飾などにより分子多様性を示すものもある．したがって，15局ではこれら医薬品は，製造方法に関する情報（構造遺伝子の由来や，製造に用いられる細胞基質の由来，遺伝子組換え法によって製造される場合は遺伝子導入法等）を記載することによって定義する方法が取られてきた．そこで基原・本質の記載については，15局の各条審議で合意が得られつつあった記載法を具体的に例示することが適当と考えられた．原薬が水溶液の場合，「水溶液」と明記すること，規格試験に分子量の項がある場合は，その規格値を明記することとする．また分子量の項がない場合では，遺伝子組換え医薬品の場合構造遺伝子の由来を記載し，遺伝子組換え糖たん白質性医薬品については，宿主細胞の種類を記載することとする．更に，ペプチド性医薬品，たん白質性医薬品，糖たん白質性医薬品，遺伝子組換え医薬品，多糖類等に分けて例示することが適当と考えられた．

2.3　含量規格について

たん白質性医薬品の含量規格の例示では，化学薬品原薬には例がないたん白質性医薬品溶液についての含量規格の記載例を示すことが適当と考えられた．

2.4　試験法の記載について

14局追補においてSDS-PAGEが参考情報に収載されて以来，主としてたん白質性医薬品を対象とする6つの試験法が局方参考情報に収載された．本研究において，これら参考情報を参照することで，試験法の簡略記載を要望する声が寄せられた．更にこれら試験法をもとに，作成要領へ記載例を作成するように要望する声が寄せられた．しかしながら，これらの試験法は参考情報であり，主として試験の原理，一般的試験方法及び注意事項の記述が主な内容となっている．また，生物薬品の場合対象物質によって，具体的試験内容は変わる場合が少なくない．したがって，これら参考情報へ収載された試験法を基に簡略記載することは，必ずしも適当ではなく，また記載例を作成するのも時期尚早と考えられた．ただし，近々の対応としては，各条での実績が生まれ，局方での経験が蓄積され，一般試験法収載が可能となった試験法は，一般試験法への収載を図ることが適切と考えられた．その候補としては，SDS-PAGE，たん白質定量法あるいはペプチドマップ法などがあげられよう．

次に，製造工程由来不純物等の記載方法の一般原則の記載についてであるが，「別に規定する」の定義についての追加説明を，作成要領に追加することが適当と考えられた．生物薬品，とりわけバイオ医薬品の多くは，ICH-Q6Bガイドラインに記されているように，規格及び試験法によるばかりでなく，製造工程の工程管理を組み合わせることによって，医薬品の品質の一定性が図られるようになっている．このような製品については，製品規格によって品質の一定性確保を図る局方への収載品にあたって，工程管理試験をどのように記載するかについてはこれからの大きな課題と考えられる．14局から「別に規定する」という記載方法が採用された理由の一つはそこにある．ただし，各条に表現されたそれぞれの意味については，局方ユーザーには理解しにくいのも確かであろう．生物薬品の製造工程に関して考慮すべき一般的事項については，今後局方の参考情報に解説を収載することが必要と思われる．更にそれとあわせて，「別に規定する」の一般原則の解説の収載についても，今後検討すべき課題となろう．

なお，平行線検定の局方での定義については，作成要領における課題というより，局方の参考情報等への収載がより相応しい対応と考えられ，これも同様に今後の局方改訂の課題の一つとなると思われる．

2.5　生物薬品と化学薬品との規格設定の違い

生物薬品の場合，エンドトキシン試験を原薬に設定する例が少なくない．参考情報のエンドトキシン規格設定値は，エンドトキシンの安全性に関して今まで得られた情報をもとに，最終製剤について定められた数値である．したがって，参考情報の設定値は，生物薬品原薬の規格値として必ずしも適当ではなく，個別には実測値をも考慮した規格値設定が合理的な場合が少なくない．このことを，作成要領の「エンドトキシン試験の設定」に説明することが適当と考えられたが，一方，局方原薬にエンドトキシ

ン試験を設定する必要性についても再度検討が必要かもしれない．

2.6 試薬・試液の記載について

生物薬品の試薬・試液についての記載範囲，あるいはキット製品の記載方法については，各条間に違いが大きく，今回の作成要領については，定まった方針をたてるに至らなかった．次回以降の検討課題としたい．

結　論

16局各条原案作成要領の生物薬品を対象とした部分の改訂のための調査を行い，問題点を整理，改訂すべきポイントを考察した．その結果，主として，構造式，分子式及び分子量，基原・本質の記載方法の整理を進めることができた．

謝　辞

本研究において，作成要領の問題点のアンケートにご協力をいただいた各社の各条原案作成担当者の皆様に感謝します．作成要領の改訂の具体的な作業は，生物薬品委員会において行われた．ただし，本報告の考察内容に関する責任は，筆者にある．

参考資料：　第16改正日本薬局方原案作成要領　生物薬品関係の改訂部分の抜粋

3.6 構造式

構造式は，「WHO化学構造式記載ガイドライン（The graphic representation of chemical formulae in the publications of international nonproprietary names (INN) for pharmaceutical substances (WHO/Pharm/95.579)", http://www.who.int/medicinedocs/collect/edmweb/pdf/h1807e/h1807e.pdf 」を指針に作成する．

ペプチド及びたん白質性医薬品のアミノ酸配列は，3文字（概ね20アミノ酸残基以下）又は1文字（概ね21アミノ酸残基以上）で表記する．また，ジスルフィド結合及び翻訳後修飾等の構造情報も明記する．ペプチド及びたん白質性医薬品については，通例，次のように記載する．

［例1］ ペプチド性医薬品

Glu-Ile-Val-Glu-Gln-Cys-Cys-Thr-Ser-Ile-Cys-Ser-Leu-Tyr-Gln-Lue-Gln-Asn

Glu1，ピログルタミン酸

［例2］ ペプチド性医薬品及びたん白質性医薬品（ヘテロダイマー）

A 鎖

OHC-MIVEQCCTSI CSLYQLENYA CGEAGFFTPE G-NH_2

B 鎖

GIVEQCIYVL LENYIALYQL PVCQHLCGSH LVAAK

B鎖：K35，プロセシング（部分的）

［例3］ ペプチド性医薬品及びたん白質性医薬品（ホモダイマー）

APAERCELAA ALAGLAFPAP RGYSLGNWVC AEPQPGGSQC VEHDCFALYP
AAKFESNFNT QATNRNTDGS TDYGILQINS GPATFLNASQ ICDGLRGHLM
RWWCNDGRTP GSRNLCNIPC SALLSSDITA TVRSSVAADA ISLLLNGDGG
SVNCAKKIVS DGNGMNAWVA WRNRCKGTDV QLPPGCGDPK RLGPLRGFQW
QAWIRGCRLV FPATCRPLAV GAWDESVENG GCEHACNAIP GAPRCQCAGP
AALQADGRSC TASATQSCND LCEHFCVPNP DQPGSYSCMC ETGYRLAADQ
HRCEDVDDCI LEPSPCPQRC VNTQGGFECH CYPNYDLVDG ECVEPVDPCF
RANCEYQCQP LNQTSYLCVC AEGFAPIPHE PHRCQMFCNQ TACPADCDPN
TQASCSCPEG YILDDGFICT DIDECENGGF CSGVCTNLPG TFECIGPDK